Modal Space Control for a Hydraulically Driven Stewart Platform

[1]Hongzhou Jiang, [2]Jingfeng He, [3]Zhizhong Tong

School of Mechatronics Engineering, Harbin Institute of Technology

No.2 Yikuang Street, Nagang District, Harbin, China

jianghz@hit.edu.cn

***Abstract*- A novel modal space controller is developed for hydraulically-driven Stewart platforms. By exploiting properties of the joint-space inverse mass matrix of hydraulically driven Stewart platforms, through a mapping of the control and feedback variables from the joint space to the decoupling modal space, the new method transforms the highly coupled six-input six-output dynamics into six independent single-input single-output (SISO) 1-DOF hydraulically driven mechanical systems. On the basis of the conventional joint space controller, a novel modal space control concept leads to a design method of modal space control with dynamic pressure feedback, which is used to solve the problem that the conventional controller could not make a damping on each degree of freedom separately. Simulation results indicate that the proposed controller is practical and yields good performance.**

Keywords- Stewart Platform; Decoupled Control; Pressure Feedback; Modal Space; Flight Simulation

I. INTRODUCTION

Hydraulically driven Stewart platforms [1] with advantages of high power-weight ratio, load carrying capacity, positioning accuracy, fast response, and high rigidity, have been widely used in various applications. A Stewart platform is a highly coupled system with complicated nonlinearities, so its control is very difficult. It is the characteristics of this mechanism that justifies the enormous attention paid to its diverse control strategies from various angles. These control strategies can be placed into two categories: joint space control (JSC) and task space control (TSC) [2], [3]. Further, these can also be divided into kinematics based control in terms of inverse and forward kinematics information, and dynamic model based control [4]-[7] which requires detailed system/model knowledge. The computed torque, inverse dynamics method and feedback linearization belong to the latter.

However, the most popular control in the industrial applications is the inverse kinematic control due to its ease of implementation and safety logic design. With this method the controller is designed in joint space, assuming that the coupling effects between the actuators are negligible or just taken as external disturbance [8]. Usually a compromise has to be found between control performance and stability, so it is difficult to improve the performance to a higher level. However it is of great industrial significance to study on a novel joint space control strategy combined with extensive system/model knowledge for hydraulically driven Stewart platforms [7].

Several researchers has investigated coupling effects between actuators by exploiting properties of the joint-space inverse mass matrix [9]-[12], thus developed some decoupled control strategies [9]-[11] for a Stewart platform.

McInroy [9], [10] proposed two decoupling algorithms by combining static input-output transformations with hexpod geometric design. Chen [11] loosened and removed severe constraints of prior decoupling methods on the allowable geometry and payload, thus greatly expanded the applications, and then proposed a decoupled control method applied to flexure-jointed hexapods for micro precision and vibration isolation applications, which have very limited stroke and no need to include typical position dependent nonlinearities.

The above control methods also can be extended to be applied to the controlling of hydraulically driven Stewart platforms, but all these require great modifications to deal with pose dependent nonlinearities and dynamics of hydraulic actuators.

Hoffman [12], however, has already showed that the hydraulically driven specific Stewart platform in any positions has six independent directions, a set of Eigen vectors, with the characteristics as described for the one degree of freedom system [4]. So it is possible to apply the methods and theories well suited for single DOF hydraulic mechanical systems to analyze and design the Stewart platform with the combination of decentralized feedback.

Plummer [13] put forward a modal control approach which can improve dynamic response of the flight simulator motion system. The modes of vibration of the system are controlled individually. These modes are dependent on the inertial properties of the platform and the compliance of the actuators.

For hydraulically driven Stewart platforms, a pressure feedback technology together with a joint space controller can be used to damp the system and to broaden the system bandwidth [8], [12]. If designing the pressure feedback in joint space, without considering coupling effects between all the actuators, even if it does work to a certain extent, one can only attenuate the resonance peaks of the lower Eigen frequencies of six rigid modes properly, and the peaking points of other relative higher Eigen frequencies will be over damped [4],[12]. So the resulting controlled system has a bandwidth corresponding to the lowest Eigen frequency [4]. This also exists in dynamic pressure feedback. Consequently this feature limits its applications significantly.

The technique presented here is an approach to design and tune the dynamic pressure feedback in decoupled modal space, and also is a proper solution to solve the above problems. With this method, each degree of freedom can be almost tuned independently and their bandwidths are totally raised near to the Eigen frequencies. Therefore the decoupled method proposed by [11],[12] is needed to transform the Stewart platform into six independent single DOF

hydraulically driven mechanical system, so this allows the dynamic pressure feedback to be designed and tuned in decoupled modal space.

II. MODELLING

In this section, the joint space dynamic model of a 6-dof electro-hydraulic Stewart platform servomechanism is developed.

A. Stewart Platform Dynamics

This is a six DOF closed kinematic chain mechanism consisting of a fixed base and a moveable platform with six electro-hydraulic actuators supporting it, see Fig.1 and Fig.2. At neutral position the body axes {M} attached to the movable platform are parallel to and coincide with the inertial frame {B} fixed to the base.

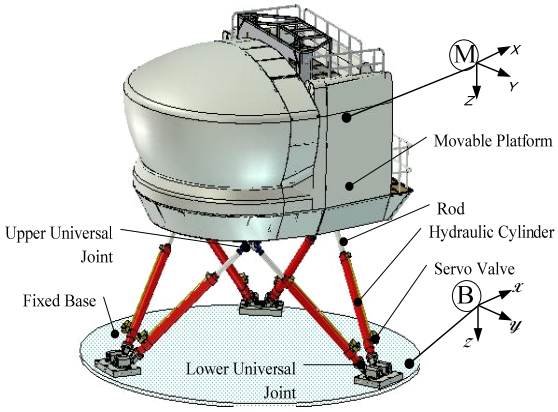

Fig. 1 Schematic view of a hydraulically driven Stewart platform

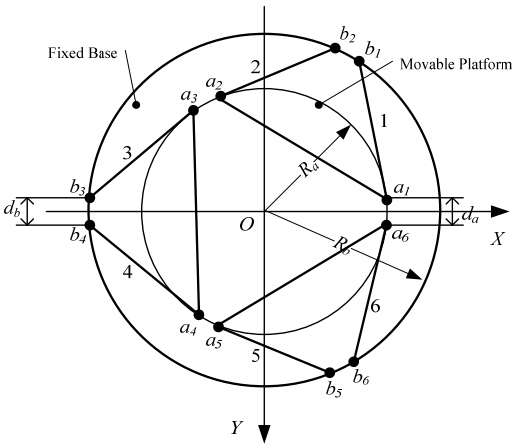

Fig. 2 Top view of a Stewart platform

The Stewart platform studied in this paper is a typical multi rigid bodies system. Without considering elasticity of all the parts, and taking upper and lower joints as ideal ones, the Stewart platform consists of fourteen rigid bodies in total. Among them thirteen bodies are movable. In Fig.2, $\mathbf{a}_i$ denotes the 3×1 vector of upper joint center point in body axes, $\mathbf{b}_i$ represents 3×1 vector of the lower joint center point in fixed base frame , and the sub index i is the actuator number.

The equations of motion of the platform are derived using Kane's method [4] and are written as

$$\mathbf{M}_t\ddot{\mathbf{q}}+\mathbf{B}_t\dot{\mathbf{q}}+\mathbf{C}_t(\mathbf{q},\dot{\mathbf{q}})\dot{\mathbf{q}}+\mathbf{G}_t=\mathbf{J}_{l,x}^{\mathrm{T}}\mathbf{f}_a \tag{1}$$

where, $\mathbf{q}=[\,x\quad y\quad z\quad \varphi\quad \theta\quad \psi\,]^{\mathrm{T}}$ is the 6×1 vector of the platform position with respect to the fixed base frame, and contains translation and Euler angles. $\dot{\mathbf{q}}$ and $\ddot{\mathbf{q}}$ are the 6×1 platform velocity vector and acceleration vector respectively, and both of them contain translation and angular components. $\mathbf{f}_a$ is the 6×1 vector of actuator output forces. $\mathbf{M}_t$ is the 6×6 mass matrix found in the base frame, and is described by Eqs.(A.1) in Appendix A with consideration of the inertial effects of the actuators. $\mathbf{B}_t$ is the viscous friction coefficients. $\mathbf{C}_t(\mathbf{q},\dot{\mathbf{q}})$ is the 6×6 Coriolis/centripetal coefficients matrix. $\mathbf{G}_t$ is the gravity terms described in detail as Eqs. (A.2) in Appendix A. $\mathbf{J}_{lx}$ is 6×6 Jacobian matrix relating the platform movements to the actuators length changes in joint space.

For ease of control analysis and design, Coulomb, Coriolis/centripetal terms are not shown in this system and neither is the gravity term. Assuming that the system is proportional damping, then Eq.(1) is simplified as

$$\mathbf{J}_{\mathrm{lx}}^{\mathrm{T}}\mathbf{f}_a=\mathbf{M}_t\ddot{\mathbf{q}} \tag{2}$$

Substituting $\mathbf{J}_{lx}\ddot{\mathbf{q}}\approx\ddot{\mathbf{l}}$ into Eq. (2), we have

$$\mathbf{f}_a=\mathbf{J}_{lx}^{-1\mathrm{T}}\mathbf{M}_t\mathbf{J}_{lx}^{-1}\ddot{\mathbf{l}} \tag{3}$$

where, $\ddot{\mathbf{l}}$ is the 6×1 acceleration vector of the actuator length changes. The mass matrix, $\mathbf{M}_{act}=\mathbf{J}_{lx}^{-1\mathrm{T}}\mathbf{M}_t\mathbf{J}_{lx}^{-1}$ known as the joint space mass matrix, as seen from the actuators contains the platform pose $\mathbf{q}$ dependent Jacobian matrix and an almost constant platform mass matrix $\mathbf{M}_t$ [4]. Then Eq. (3) is rewritten as

$$\mathbf{M}_{act}^{-1}\bar{\mathbf{f}}_a=\mathbf{J}_{lx}\mathbf{M}_t^{-1}\mathbf{J}_{lx}^{T}\bar{\mathbf{f}}_a=\ddot{\bar{\mathbf{l}}} \tag{4}$$

This Joint Space mass matrix determines the coupling effects between the actuators. Since the mass matrix is symmetric the eigenvector matrix can be made unitary. This results from the singular value decomposition

$$\mathbf{M}_{act}^{-1}=\mathbf{U}\boldsymbol{\Sigma}\ \mathbf{U}^{\mathrm{T}} \tag{5}$$

where, $\boldsymbol{\Sigma}=\mathrm{diag}\left(\left[\sigma_1\quad\sigma_2\quad\sigma_3\quad\sigma_4\quad\sigma_5\quad\sigma_6\right]^{\mathrm{T}}\right)$ are singular values, and $\mathbf{U}$ is a pose dependent unitary orthogonal matrix. One can get its linearised version for ease of real time implementation, under the assumption that all six actuators are identical and have the same mass, damping and stiffness, i.e. at neutral position all other matrix is a scalar times an identity matrix. This still holds if decentralized (diagonal feedback structure) is applied [4].

B. Hydraulic Modeling in Joint Space

In this section, the basic structure of a hydraulically driven Stewart platform is given in Fig.3. The hydraulic servo valves are simplified as proportional gains under an assumption that their frequency bandwidths are far beyond the hydraulic actuators. With the consideration of the servo valve flow rate, leakage, hydraulic capacity, piston movement etc., the flow continuity of the chambers of the actuators is also shown here. The payload pressure P_L, derived from the pressurization of the hydraulic actuators, acts on the effective operational area A_p of the actuators, and generates the forces to move the

platform. The dynamic model of a Stewart platform described by Eq. (4) in joint space, is included here. The gravity term is considered and transformed into joint space by Jacobian matrix. The Coriolis/centripetal nonlinear terms are not included in this structure, which will be taken as uncertain external disturbance in control design. Here the system characteristics will be analyzed through linearization at neutral position and a decoupling transformation. Considering

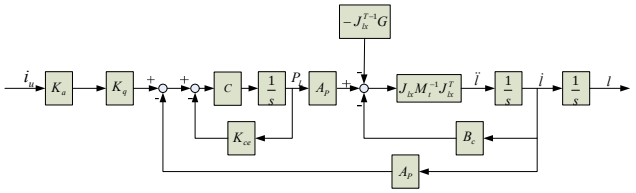

Fig. 3 Joint space dynamic model of a hydraulically driven Stewart platform

Eq. (4), the dynamic characteristics of the i^{th} actuator, we can get

$$\sum_{j=1}^{6}\mathbf{M}_{act}^{-1}(i,j)f_{a,j}=\ddot{l}_i \tag{6a}$$

where $\mathbf{M}_{act}^{-1}(i,j)$ represents the element at the ith row and jth column of the inverse mass matrix in joint space, $f_{a,j}$ is a scalar describing the output force of actuator j, $\ddot{l}_i$ is a scalar denoting the acceleration of the ith actuator length changes, and $i,j=1,2\cdots 6$.

Taken Laplace transforms, the flow continuity equation of the jth actuator is

$$k_a k_q i_{u,j}=l_j A_p s+\left(\frac{1}{c}s+k_{ce}\right)P_{L,j} \tag{6b}$$

where, k_a is the control gain, k_q , $i_{u,j}$ are the flow rate coefficient and input current of the servo valve respectively, l_j , A_p , c , k_{ce} , $P_{L,j}$ are the length, operational area, hydraulic capacity, general ratio of flow rate to pressure, payload pressure of the actuator, the sub index j stands for the actuator number, s is Laplace derivative operator.

The net output force of the jth actuator is given as

$$f_{a,j}=A_p P_{L,j}-b_c l_j s \tag{6c}$$

where, b_c is the viscous damping coefficient.

Rearranging Eq. (6b), the pressurization of the jth actuator chamber can be described by

$$P_{L,j}=\frac{k_a k_q i_{u,j}-l_j A_p s}{\frac{1}{c}s+k_{ce}} \tag{6d}$$

Combining Eqs. (6a-6d), we have the dynamic equations in joint space as

$$\sum_{j=1}^{6}M_{act}^{-1}(i,j)\left[\frac{k_a k_q i_{u,j}/A_p-s\left(1+\frac{b_c k_{ce}}{A_p^2}+\frac{b_c}{cA_p^2}s\right)l_j}{\frac{1}{cA_p^2}s+\frac{k_{ce}}{A_p^2}}\right]=l_i s^2 \tag{7}$$

Further the dynamic math model of all the six actuators is written as

$$s\left[s\left(s\frac{1}{cA_p^2}+\frac{k_{ce}}{A_p^2}\right)\mathbf{E}_{6\times 6}+\left(1+\frac{b_c k_{ce}}{A_p^2}+\frac{b_c}{cA_p^2}s\right)\mathbf{M}_{act}^{-1}\right]\mathbf{l}=k_a k_q\mathbf{M}_{act}^{-1}\mathbf{i}_u/A_p \tag{8}$$

where, $\mathbf{E}_{6\times 6}$ is a 6×6 identity matrix, $\mathbf{i}_u=\left(i_{u,j}\right)$, $\mathbf{l}=\left(l_j\right)$ with $j=1,2\cdots 6$. Defining the new variables $\hat{\mathbf{l}}=\mathbf{U}^{\mathrm{T}}\mathbf{l}$, $\hat{\mathbf{i}}_u=\mathbf{U}^{\mathrm{T}}\mathbf{i}_u$, substituting them into Eq.（8）, the dynamic model in modal space is given by

$$s\left[s^2\frac{1}{cA_p^2}\mathbf{E}_{6\times 6}+s\left(\frac{b_c}{cA_p^2}\mathbf{E}_{6\times 6}+\frac{k_{ce}}{A_p^2}\mathbf{\Sigma}\right)+\left(1+\frac{b_c k_{ce}}{A_p^2}\right)\mathbf{\Sigma}\right]\hat{\mathbf{l}}=k_a k_q\mathbf{\Sigma}\hat{\mathbf{i}}_{\mathbf{u}}/A_p \tag{9}$$

Defining $\mathbf{C}=c\mathbf{E}_{6\times 6}$, $\mathbf{B}_{\mathrm{c}}=b_{\mathrm{c}}\mathbf{E}_{6\times 6}$, $\mathbf{K}_{ce}=k_{ce}\mathbf{E}_{6\times 6}$, $\mathbf{K}_{\mathrm{q}}=k_q\mathbf{E}_{6\times 6}$ and $\mathbf{K}_{\mathrm{a}}=k_a\mathbf{E}_{6\times 6}$, Eq.9 can be rewritten into a more generalized form.

$$s\left[s^2\frac{1}{A_p^2}\mathbf{C}^{-1}+s\left(\frac{1}{A_p^2}\mathbf{C}^{-1}\mathbf{B}_c+\frac{1}{A_p^2}\mathbf{K}_{ce}\mathbf{\Sigma}\right)+\left(\mathbf{E}_{6\times 6}+\frac{1}{A_p^2}\mathbf{B}_c\mathbf{K}_{ce}\right)\mathbf{\Sigma}\right]\hat{\hat{\mathbf{l}}}=\mathbf{K}_a\mathbf{K}_q\mathbf{\Sigma}\hat{\hat{\mathbf{i}}}_{\mathbf{u}}/A_p \tag{10}$$

So along with the modal directions, the system is decoupled into six third-order subsystems in parallel, each of them consisting of one integrator in series with one second-order system and having the same form as a single DOF hydraulically driven mechanical system. Then the ith order rigid mode can be described by

$$s\left[s^2\frac{1}{cA_p^2\sigma_i}+s\left(\frac{b_c}{cA_p^2\sigma_i}+\frac{k_{ce}}{A_p^2}\right)+\left(1+\frac{b_c k_{ce}}{A_p^2}\right)\right]\hat{l}_i=k_a k_q\hat{i}_{u,i}/A_p \tag{11}$$

Since usually the term $\frac{b_c k_{ce}}{A_p^2}\ll 1$, thus the undamped Eigen frequencies ϖ_h can be considered according to the rigid modes and mainly determined by the hydraulic capacity, c, and the singular values of the inverse mass matrix, $\mathbf{\Sigma}$.

$$\varpi_h=A_p\sqrt{c}\left(\left[\sqrt{\sigma_1}\quad\sqrt{\sigma_2}\quad\cdots\quad\sqrt{\sigma_6}\right]^T\right) \tag{12}$$

These singular values can be interpreted as the inverse of the generalized masses, which the actuators will have to accelerate in moving along the six orthogonal directions described by the columns of the unitary decoupling matrix U [4].

So far, with decoupled six SISO systems, it is possible to apply the methods and theories well suited to a single DOF hydraulic mechanical system to analyze and design the Stewart platform with the combination of decentralized feedback.

For a single DOF hydraulically driven mechanical system with only mass payloads, its open loop transfer function is a type I system with respect to input signals, and a type 0 system with respect to external disturbing forces [15]. Therefore, the tracking error $\Delta Y(s)$ of each decoupled channel, caused by inputs $R_p(s)$ and external disturbance forces $F(s)$, can be described by

$$\Delta Y_i(s)=\Phi_{e,i}(s)R_{p,i}(s)+\Phi_{ef,i}(s)F_i(s) \tag{13}$$

with,

$$\Phi_{e,i}(s)=\frac{s\left(\frac{1}{\varpi_{h,i}^2}s^2+\frac{2\varsigma_{h,i}}{\varpi_{h,i}}s+1\right)}{s\left(\frac{1}{\varpi_{h,i}^2}s^2+\frac{2\varsigma_{h,i}}{\varpi_{h,i}}s+1\right)+\hat{k}_{a,i}k_q}$$

$$\Phi_{ef,i}=-\frac{Y_i}{F_i}=\frac{k_{ce}/A_p^2\left(1+\frac{1}{ck_{ce}}s\right)}{s\left(\frac{1}{\varpi_{h,i}^2}s^2+\frac{2\varsigma_{h,i}}{\varpi_{h,i}}s+1\right)+\hat{k}_{a,i}k_q}$$

where, $\hat{k}_{a,i}$ is a scalar denoting the proportional gain in modal space. The steady state errors caused by external disturbance force can be described with

$$-\frac{Y_i}{F_i} = \frac{k_{ce}}{\hat{k}_{a,i} k_q A_p^2} \tag{14}$$

Theoretically, if external disturbance, such as gravity, can be fully compensated, a proportional position control is sufficient to achieve a performance without position errors, since each decoupled channel is a type I system. To ensure that the system is stable and has enough stability margins, the forward gain should satisfy the following inequality constraints [15].

$$\hat{k}_{a,i} < \varsigma_{h,i} \varpi_{h,i} A_p / k_q k_f \tag{15}$$

where, k_f is a scalar denoting the position feedback gain.

III. CONTROL DESIGN

In this section, first a 1-dof hydraulically driven mechanical system is introduced and dynamic pressure feedback compensation is discussed. Second, two control strategies for a Stewart platform, including a joint space control and a modal space control, are summarized.

A. Dynamic Pressure Feedback for 1-Dof Hydraulically Driven Mechanical System

Now that the system has been decoupled into six SISO third order systems, it seems worthwhile to review a hydraulic actuator driving a mass. The linearised version from valve input to actuator position consists of a slightly damped second order system in series with an integrator. When controlled with proportional position feedback, only low performance can be obtained. To achieve higher bandwidth, the resonance of second order system has to be damped sufficiently. This can be done by pressure feedback [14], [15]. But the inner loop with pressure difference feedback will decrease the rigidity of the system. To solve this problem, an alternative method can be applied using dynamic pressure feedback, in which pressure difference feedback signals are filtered by a one-order high pass band filter [15].

According to the analysis of [15], the dynamic pressure feedback correction is equivalent to an acceleration feedback without changing the undamped Eigen frequency ω_{hi}. In this manner a closed loop bandwidth approximately equal to ω_{hi} can be attained.

Defining that ξ_h is the original damping ratio and ξ_h'' is the desired damping ratio, and then the dynamic pressure feedback gain k_{dp} can be calculated by

$$k_{dp} = \frac{2(\xi_h'' - \xi_h) \cdot \sigma_i A_p^{\ 2}}{k_{a,i} k_q \omega_{hi}} \tag{16}$$

The cutting frequency of the high pass filter is assigned with $\omega_{hi}/3$. A compromise of the damping ratio has to be achieved, because the damping ratio with higher value will also decrease the close loop bandwidth.

B. Joint Space Controller

A conventional joint space controller for a hydraulically driven Stewart platform consists of an inverse kinematics block and a position servo controller of hydraulic actuators. The control structure is shown in Fig. 4. The controller is a position control loop with proportional gains and it is designed in joint space with neglecting the coupling effects of all the actuators. The dynamic pressure feedback correction is also included to damp the hydraulic resonance peaks. This control strategy is very easy to implement, because there is no need to have much more knowledge about dynamic models. This can explain its popularity in industrial applications in spite of its poor performance.

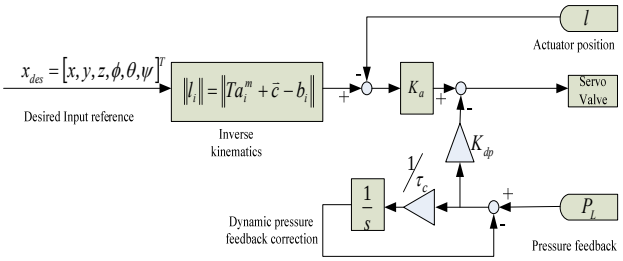

Fig. 4 Joint space control with dynamic pressure feedback compensation

In Fig. 4, the input reference signals are desired platform positions which are used to calculate actuator lengths commands through an inverse kinematics block, then sent to the servo controllers, in which there are three parameters required to be tuned, they are the proportional gain $\mathbf{K}_a$, cutting frequency $1/\boldsymbol{\tau}_c$ and dynamic pressure feedback coefficient $\mathbf{K}_{dp}$. One can tune these parameters repeatedly until the expected performance is achieved according to one's experiences.

C. Modal Space Controller

The structure of the modal space controller as shown in Fig.5 is very similar to the conventional joint space control, however the signals including control errors, control outputs and pressure difference feedbacks are transformed into the decoupled modal space by the unitary decoupling matrix, U, so the coupling effects between all the actuators are fully considered. The proportional gains and dynamic pressure feedback functions are also tuned in modal space.

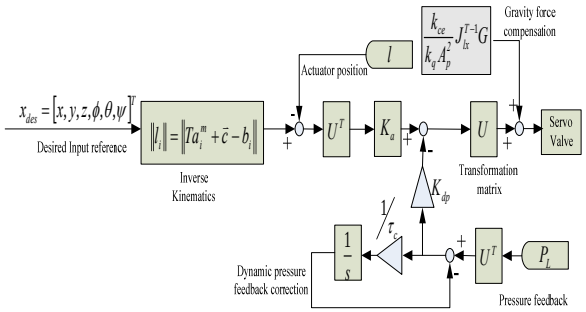

Fig. 5 Modal space control with gravity compensation

The calculation of the unitary decoupling matrix is not shown in Fig.5, but this does not mean that it's the least. In addition, the identification of the inertial parameters is needed to support the control algorithm fulfilment. The unitary decoupling matrix, U, will be chosen from the simplified linearised version at neutral position to the more complicated pose dependent one. The choosing criterion is to ensure both good performance and facilitating the real time implementation. In steady state, according to Eq. (14), the term of gravity compensation added at the controller output is

written as $\frac{k_{ce}}{k_q A_p^2}\mathbf{J}_{lx}^{\mathrm{T}-1}\mathbf{G}$, so the steady errors caused by gravity can be reduced to almost zero [16]. So the control inputs of the servo valves can be expressed as

$$\begin{aligned}\mathbf{i}_u &= \mathbf{U}\,\mathrm{diag}\left(\begin{bmatrix}\mathrm{k}_{a,1} & \mathrm{k}_{a,2} & \cdots & \mathrm{k}_{a,6}\end{bmatrix}^{\mathrm{T}}\right)\mathbf{U}^{\mathrm{T}}\mathbf{e}\\ &\cdots+\mathbf{U}\,\mathrm{diag}\left(\begin{bmatrix}\mathrm{k}_{dp,1}\frac{\tau_{c,1}\mathrm{s}}{\tau_{c,1}\mathrm{s}+1} & \mathrm{k}_{dp,2}\frac{\tau_{c,2}\mathrm{s}}{\tau_{c,2}\mathrm{s}+1} & \cdots & \mathrm{k}_{dp,6}\frac{\tau_{c,6}\mathrm{s}}{\tau_{c,6}\mathrm{s}+1}\end{bmatrix}^{\mathrm{T}}\right)\mathbf{U}^{\mathrm{T}}\mathbf{P}_{\mathrm{L}}\\ &\cdots+\frac{k_{ce}}{k_q A_p^2}\mathbf{J}_{lx}^{\mathrm{T}-1}\mathbf{G}\end{aligned} \tag{17}$$

where, the position error $\mathbf{e}=\mathbf{l}_{\mathrm{com}}-\mathbf{l}=\left(e_j\right)$, the unitary decoupling matrix $\mathbf{U}=\left(U_{jk}\right)$, the payload pressure $\mathbf{P}_{\mathrm{L}}=\left(P_{Lj}\right)$, the Jacobian matrix $\mathbf{J}_{lx}=\left(J_{ij}\right)$, the gravity term $\mathbf{G}=\left(G_j\right)$ with $i,j,k=1,2\cdots6$, $\mathbf{l}_{\mathrm{com}}$ is the actuator length command in terms of inverse kinematics.

For the ease of programming, each element of $\mathbf{i}_u$ in Eq. (17) is given here as

$$i_{u,i}=\sum_{j=1}^{6}\left(\left(\sum_{k=1}^{6}U_{ik}U_{jk}k_{a,k}\right)e_j+\left(\sum_{k=1}^{6}U_{ik}U_{jk}k_{dp,k}\frac{\tau_{c,k}s}{\tau_{c,k}s+1}\right)P_{Lj}+\frac{k_{ce}}{k_q A_p^2}J_{ij}G_j\right) \tag{18}$$

Analyzing Eqs.(17,18), when $k_{a,1}=k_{a,2}=\cdots=k_{a,6}$ and $k_{dp,1}=k_{dp,2}=\cdots=k_{dp,6}$, the modal space controller degenerates into the conventional counterpart.

IV. SIMULATION RESULTS

In this section, two control strategies applied to a flight simulator motion system are evaluated. Its configuration parameters are shown in Table 1.

TABLE I

CONFIGURATION PARAMETERS

	Descriptions	Values	Units
R_a	Distribution Radius of Upper Joint Points	2.1148	m
R_b	Distribution Radius of Lower Joint Points	2.5170	m
h	Platform Height in Neutral Position	2.6519	m
m_s	Payload Mass	13642.000	kg
I_{XX}	Moment of Inertia	46477.100	kg m^2
I_{YY}	Moment of Inertia	49396.100	kg m^2
I_{ZZ}	Moment of Inertia	53865.000	kg m^2
X_{cg}	X Component of Mass Center Position	0.000	m
Y_{cg}	Y Component of Mass Center Position	0.000	m
Z_{cg}	Z Component of Mass Center Position	-1.772	m
d_a	Short Section of Upper Platform	0.2286	m
d_b	Short Section of Fixed Base	0.2285	m

The setup parameters of hydraulic actuators are shown in Table 2.

TABLE II

HYDRAULIC ACTUATOR SETUP PARAMETERS

	Descriptions	Values	Units
i_a	Inertia of Actuator Upper Part around Gimbal Point	76.12	kg m^2
i_b	Inertia of Actuator Lower Part around Gimbal Point	25.13	kg m^2
m_a	Mass of Actuator Upper Part	50.34	kg
m_b	Mass of Actuator Lower Part	152.69	kg
r_a	Mass Center Position of Actuator Upper Part Relative to Upper Gimbal Point	0.993	m
r_b	Mass Center Position of Actuator Lower Part Relative to Lower Gimbal Point	0.993	m
k_q	Discharge Flow Ratio of Servo Valve	0.00064	m^3/s/A
P_s	Supply Pressure	12	MPa
Q_N	Max. Valve Flow	0.0064	m^3/s
c	Hydraulic Stiffness	92564	MPa/ m^3
A_p	Operational Area	0.0099	m^2
b_c	Viscous Friction Coefficient	7000	N s m^{-1}
k_{ce}	General Ratio of Flow Rate to Pressure	6.6564e-11	m^3/s /Pa

The undamped Eigen frequencies of the motion system as shown in Table 3 are calculated using Eq. (11).

TABLE III

EIGEN FREQUENCIES

	Modal direction	Hydraulic Eigen Frequency (Hz)
1.	(*-y,rx*) Negative Lateral Motion and Positive Roll	9.326
2.	(*-x,-ry*) Negative Longitudinal Motion and Negative Pitch	9.088
3.	*-z* , Heave	7.842
4.	*Rz* , Yaw	6.433
5.	(*-y,-rx*) Negative Lateral Motion and Negative Roll	2.912
6.	(*x,-ry*) Positive Longitudinal Motion and Negative Pitch	2.896

The simulation model is built in Simulink®. It consists of six blocks on top level. The first is a signal generator used to generate platform trajectories, such as square waves, sine waves and band limited white noises. The second is the inverse kinematics block used to calculate the actuators commands with respect to platform trajectories. The third is the hydraulic system block including controller and hydraulic actuators model. The fourth is the plant block representing the equations of motion built using SimMechanics®, a proven copy referring to a demo provided by the Mathworks, Inc, with considering actuators inertial effects, gravity and Coriolis/centripetal forces. This means that the nonlinearities neglected in control analysis and design, are reconsidered in simulation stage. The fifth is the forward kinematics block used to compute the platform positions from the measured actuator lengths in real time, and its algorithm has been proven right and practical in reference [4]. The sixth is the inverse dynamics block used to calculate the unitary decoupling matrix, U and gravity compensation terms, and its algorithm is shown in Appendix A. Although that can also be found in literature [4], a slight modification is made by just considering additional inertial contributions of the lower parts rotation of the actuators.

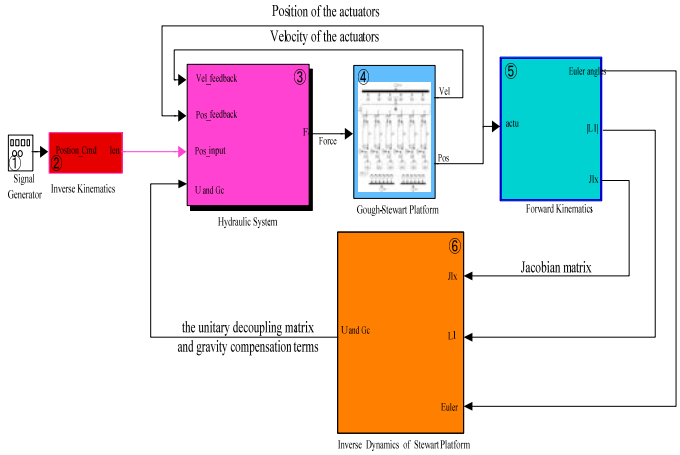

Fig. 6 Block diagram of the hydraulically driven Stewart platform

Next, the resulting performance characteristics of the motion system will be outlined. The describing function enables the characterization of some of the parameters, which are considered most important in control, like bandwidth, damping, and interaction in multivariable system [4]. Both the amplitude and phase frequency characteristics of the motion system from 0.5 to 40 Hz are shown in figures. Direct comparison of both the modal space controller and the conventional controller is also given.

The Bode plots of the closed loop system from the desired to actual positions applying the basically conventional control strategy and the modal space controller at the neutral position are shown in Fig.7 and Fig.8.

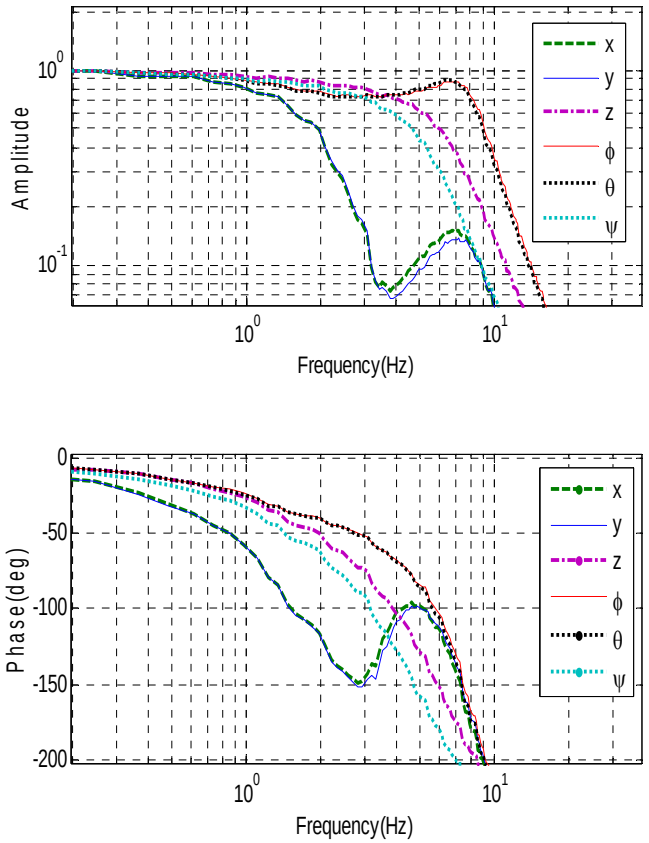

Fig. 7 Frequency response of the modal space controlled motion system

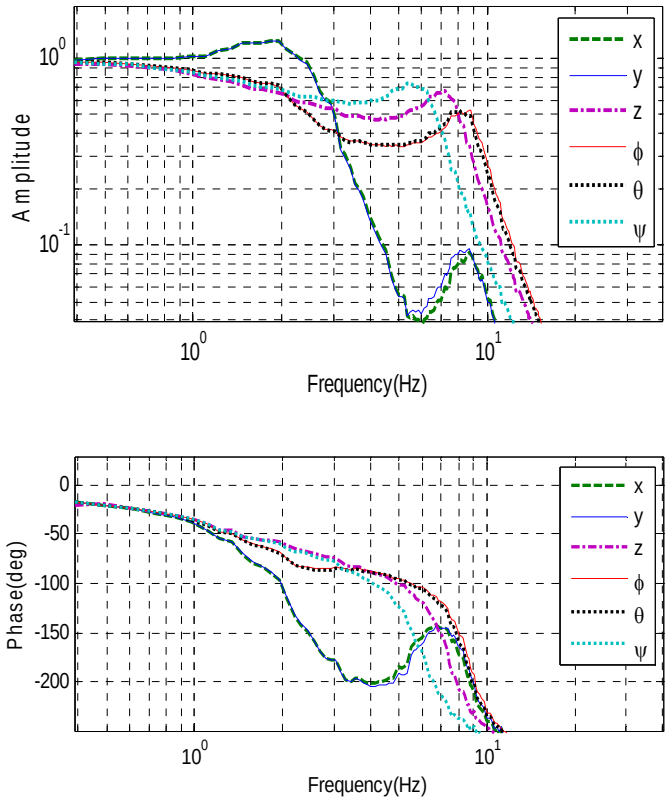

Fig. 8 Frequency response of the conventionally controlled motion system

For the modal space control, it can be seen in Fig.7 that the -3dB point can be found at 8 Hz for pitch (ry) and roll (rx), 4 Hz for heave (z), 3Hz for yaw. In surge(x) and sway(y) the bandwidth is just only 1.5 Hz which is the lowest compared to other directions. The -90 deg bandwidth can be found at 5 Hz for pitch (ry) and roll (rx), 3.5 Hz for heave (z), 3Hz for yaw (rz), 1.5 Hz for surge(x) and sway(y). The highest bandwidths are attained with pitch (ry), roll (rx) and somewhat lower with heave (z). All responses are reasonably flat without peaking more than a few percent above 0 dB.

For reference purposes, a conventional approach was used to control the same motion system. The frequency response is given in Fig.8. Since there is no compensation for different natural frequencies, some responses, like surge (x) and sway (y), demonstrate peaks much more than others (such as pitch (ry) and roll (rx), which are over damped). Except for surge and pitch, the bandwidth is as low as 1.5Hz.

As expected, with the conventional controller it is impossible to tune the bandwidths of the platform position loops on each degree of freedom separately. Furthermore, a compromise has to be found between peaking (up till 3 dB) of the lowest bandwidth loops of surge (x) and sway (y) and the over damped response of pitch (ry) and roll (rx). The 2 Hz bandwidth of roll (rx) and pitch (ry) is also a maximum attainable bandwidth using this control structure being limited by the lowest Eigen frequency of the platform.

With the conventional controller the bandwidth of x and y is 2.5Hz attainable, higher than that with the modal space controller, which is only 1.5Hz. It seems to give an impression that the dynamic performance along these degrees of freedom is deteriorated using the novel controller. In fact, the bandwidth of the conventional control is achieved at the expense of higher overshoot and poor performances of the

other degrees of freedom. The bandwidth of the modal space controller can be tuned to a higher level, as the same as the conventional control, but that will not meet the requirements of a flight simulator motion system in which flat frequency response is preferable. On the contrary, with the modal space controller, obviously each degree of freedom can be almost tuned independently, and their bandwidths are totally raised near to the Eigen frequencies. Particularly the roll and pitch are improved from 2Hz to 8Hz, yaw is raised from 2Hz to 3Hz, and the heave increased from 1.5Hz to 4Hz. The comparison of two control strategies indicates that the modal space control is superior to the conventional.

Transients' response results as shown in Fig.9-10 are also provided here to show characteristics of the system in time domain. Step inputs are fed into the system along each DOF in proper sequence. Inputs amplitude is 1 deg along the rotation axes and 3 mm along the translation axes respectively.

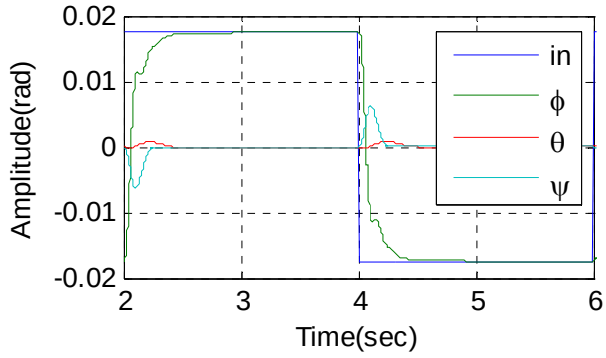

a) roll

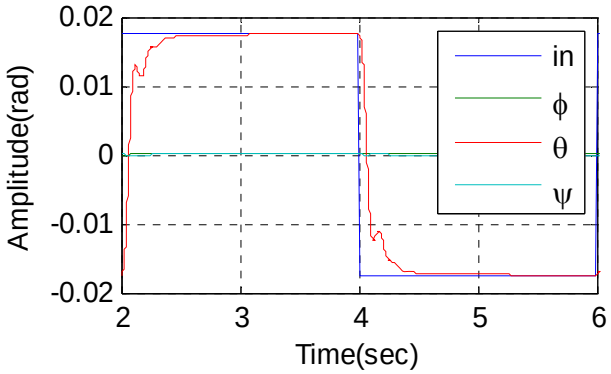

b) pitch

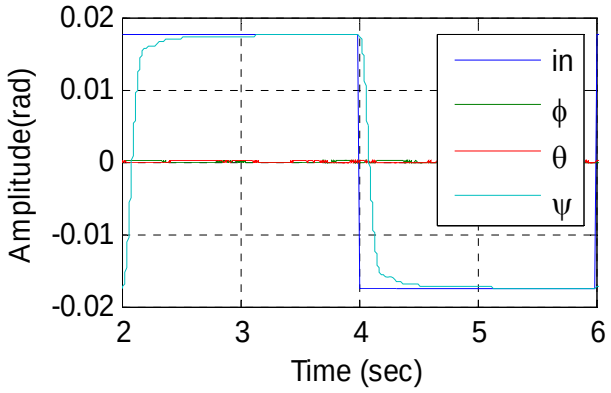

c) yaw

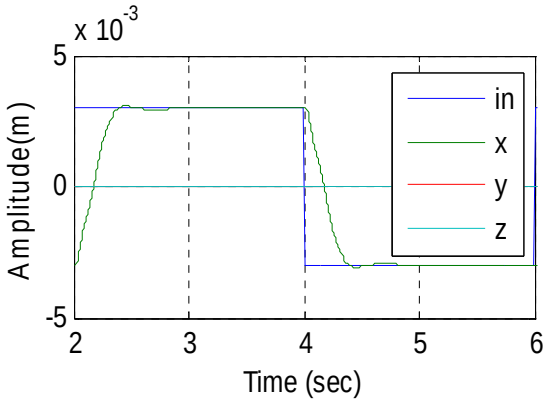

d) surge

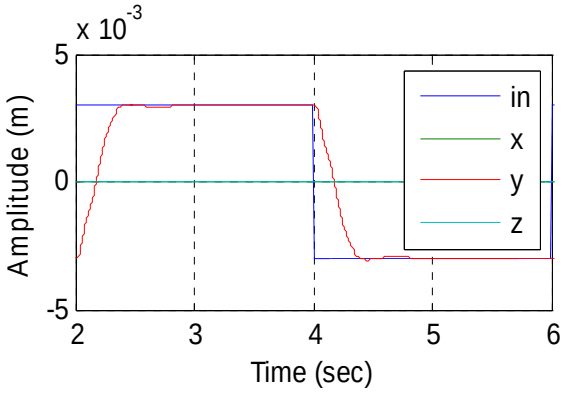

e) sway

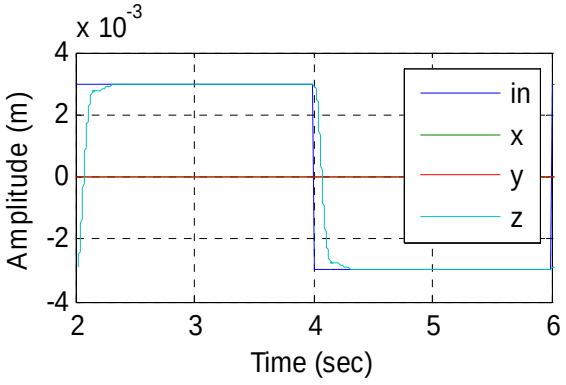

f) heave

Fig. 9 Short time response with step position inputs of Tthe modal space control

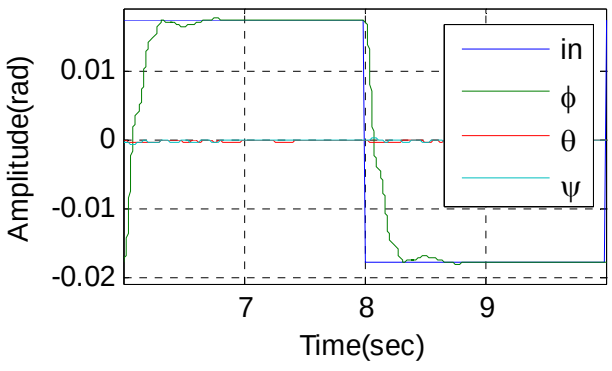

a) roll

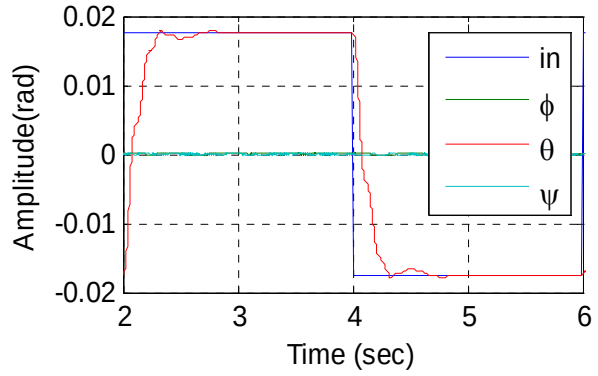

b) pitch

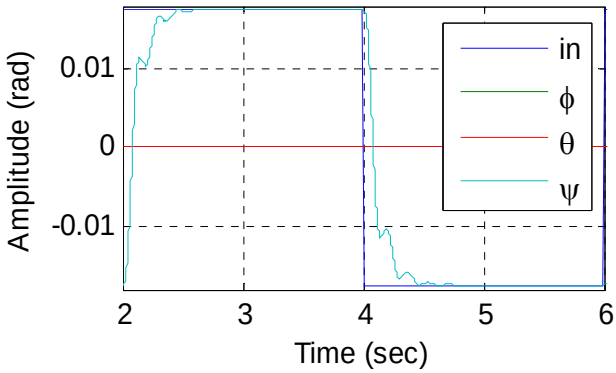

c) yaw

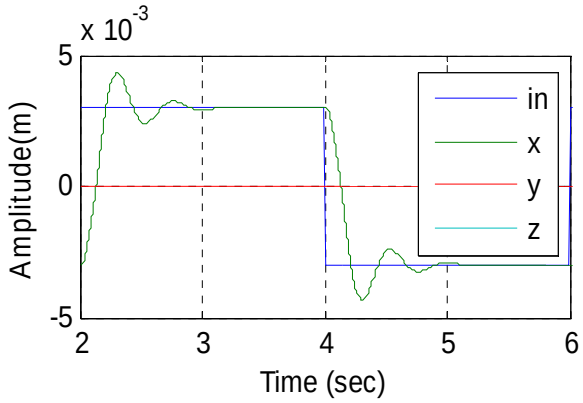

d) surge

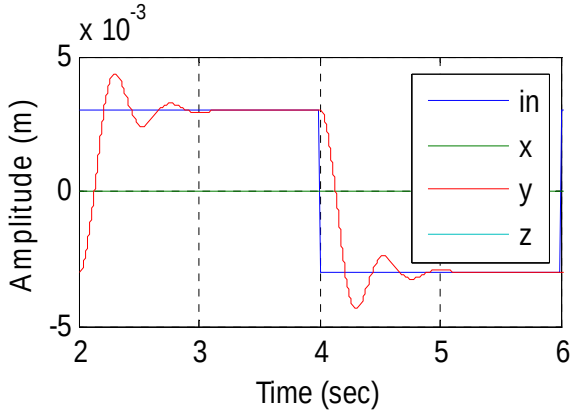

e) sway

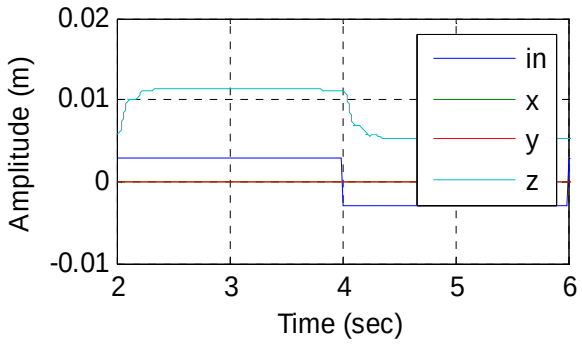

f) heave

Fig. 10 Short time response with step position inputs of the conventional control

The simulation results show that it is very effective to design and tune the system in modal space, and the bandwidth is increased dramatically except surge (x) and sway (y) motions. However the system bandwidth is still limited by the hydraulic Eigen frequencies. Some other methods are required to be introduced to broaden the system bandwidth further. Maybe a velocity feedback in modal space is a candidate solution.

In addition, there are still some open issues about putting the modal space controller into practice. First, to avoid modelling errors violating the dynamic performance, practical and effective model parameters identification technologies, including geometrical structure, inertial parameters, and configuration parameters of the hydraulic actuators, are needed. Secondly, some tests and trials are required to find a trade-off between model complexities and feasibility of real time code implementation. Third, the effects of transmission line dynamics on the dynamic pressure feedback can not be ignored in practice [17], [18].

V. CONCLUSIONS

By making a singular values decomposition of the joint-space inverse mass matrix of a hydraulically driven Stewart platform and mapping the control and feedback variables from the joint space to the decoupling modal space, the highly coupled six-input six-output dynamics can be transformed into six independent single-input single-output (SISO) 1-DOF hydraulically driven mechanical systems. So it is possible to use the design and control methods well suited for 1-DOF hydraulically driven mechanical systems to deal with Stewart platforms.

Generally, the proportional control together with dynamic pressure feedback correction is used in industrial applications. It is impossible to achieve good performance by just using the conventional joint space control in which coupling effects between all the actuators are not considered thoroughly. The simulation results indicate that the conventional controller can only attenuate the resonance peaks of the lower Eigen frequencies of six rigid modes properly, and the peaking points of other relative higher Eigen frequencies are overly damped. So the system bandwidth is limited by the lower Eigen frequencies.

To solve the above problems, a novel modal space controller with dynamic pressure feedback correction is developed. Though the structure of a modal space controller is very similar to the conventional joint space control, the

signals including the control errors, control outputs and pressure feedbacks are transformed into the decoupled modal space. The proportional gains and dynamic pressure feedback parameters are also tuned in modal space. With this method each degree of freedom can be almost tuned independently and their bandwidths are totally raised near to the Eigen frequencies. The simulation results indicate that, in comparison with the conventional joint space controller, the modal space controller is practical and can improve the dynamic performance of each degree of freedom.

ACKNOWLEDGEMENTS

This work is financially supported by the National Natural Science Foundation of China (Grant No. 50975055 and Grant No. 51175100).

APPENDIX A

Considering inertial effects of all the actuators of a Stewart platform, the mass matrix is described by

$$\mathbf{M}_t = \mathbf{M}_{\bar{c}} + \sum_{i=1}^{6} \mathbf{J}_{\mathbf{a}_i,x}^T \left(\mathbf{M}_{\mathbf{a}_i} + \mathbf{M}_{b_i} + \mathbf{M}_{i_{a,i},i_{b,i}} \right) \mathbf{J}_{a_i,x} \tag{A.1}$$

with,

$$\mathbf{M}_{\bar{c}} = \begin{bmatrix} \mathrm{m_s}\mathbf{I} & \bar{\mathbf{0}}_{3\times3} \\ \bar{\mathbf{0}}_{3\times3} & \mathbf{I}_c \end{bmatrix}$$

$$\mathbf{M}_{\mathbf{a}_i} = m_{\mathbf{a}_i} \left(\mathbf{I} - \mathbf{P}_{\mathbf{l}_{n,i}} + \frac{\left(|\mathbf{l}_i| - r_{\mathbf{a}_i} \right)^2}{|\mathbf{l}_i|^2} \mathbf{P}_{\mathbf{l}_{n,i}} \right)$$

$$\mathbf{M}_{\mathbf{b}_i} = m_{\mathbf{b}_i} \frac{r_{\mathbf{b}_i}^{\ 2}}{|\mathbf{l}_i|^2} \mathbf{P}_{\mathbf{l}_{n,i}}$$

$$\mathbf{M}_{i_{a,i},i_{b,i}} = \frac{\left(i_{a_i} + i_{b_i} \right)}{|\mathbf{l}_i|^2} \mathbf{P}_{l_{n,i}}$$

$$\mathbf{J}_{\mathbf{a}_i,\mathbf{x}} = \begin{bmatrix} \mathbf{I} & \mathbf{T} \left(\tilde{\mathbf{A}}_i^m \right)^{\mathrm{T}} \mathbf{T}^{\mathrm{T}} \end{bmatrix}$$

$$\mathbf{P}_{\mathbf{l}_{n,i}} = \mathbf{I} - \mathbf{l}_{n,i} \mathbf{l}_{n,i}^{\mathrm{T}}$$

where, $\mathbf{l}_i$ is the 3×1 vector between the upper and lower gimbal points of an actuator, $\mathbf{l}_{n,\mathrm{i}}$ is the 3×1 unit vector of $\mathbf{l}_i$, $\mathbf{T}$ is the rotation matrix, $\tilde{\mathbf{A}}_i^m$ is a skew symmetric matrix of the vector $\mathbf{a}_\mathrm{i}$, m_{a_i} and m_{b_i} are the upper part mass and lower part mass of an actuator respectively, r_{a_i} is the distance from upper joint point to the mass centre of the actuator upper part, r_{b_i} is the distance from lower joint point to the centre of mass of the actuator lower part, i_{a_i} and i_{b_i} are scalar values representing inertia moments of upper part and lower part of actuators around gimbal point .

The gravity terms of the gross payload of the platform can be given as

$$\mathbf{G}_t = \mathbf{G}_{\bar{c}} + \sum_{i=1}^{6} \mathbf{J}_{\mathbf{a}_i,\mathbf{x}}^{\mathrm{T}} \left(\mathbf{G}_{m_{a_i}} + \mathbf{G}_{m_{b_i}} \right) \tag{A.2}$$

with,

$$\mathbf{G}_{\bar{c}} = \begin{bmatrix} m_s \mathbf{g}^{\mathrm{T}} & \bar{\mathbf{0}}_{1\times3} \end{bmatrix}^{\mathrm{T}}$$

$$\mathbf{G}_{m_{a_i}} = m_{a_i} \left(\mathbf{I} - \frac{r_{a_i}}{|\mathbf{l}_i|} \mathbf{P}_{\mathbf{l}_{n,i}} \right) \mathbf{g}$$

$$\mathbf{G}_{m_{b_i}} = m_{b_i} \frac{r_{b_i}}{|\mathbf{l}_i|} \mathbf{P}_{\mathbf{l}_{n,i}} \mathbf{g}$$

where, g is the gravity acceleration vector.

Although Eqs.(A.1-A.2) can also be found in [4], a slight modification is made here by just considering additional inertial contributions of lower parts rotation of actuators, which has been ignored in [4].

APPENDIX B

The forward kinematics has been tackled numerically by performing the Newton-Raphson (NR) iteration scheme [4] given as

$$\mathbf{q}_{k+1} = \mathbf{q}_k + \mathbf{J}_{l,sx}^{-1}(\mathbf{q}_k)(\mathbf{l}_{measured} - \mathbf{l}_k) \tag{B.1}$$

where k is iteration number, $\mathbf{l}_{measured}$ are measured actuator lengths. We should take note of $\mathbf{J}_{l,sx}$ different from $\mathbf{J}_{l\mathrm{x}}$. The convergence conditions of NR-iteration of Eq. (B.1) have been investigated and proven in [4].

REFERENCES

[1] Stewart, A platform with six degrees of freedom, in: Proceedings of the IMechE, vol. 180, Pt. 1, No. 15, 1965–1966, pp. 371–385.

[2] K. Liu, M. Fitzgerald, D.W. Dawson, F.L. Lewis, Control of Systems with Inexact Dynamic Models ASME-33 (1991) 83-89.

[3] B. Dasgupta, T.S. Mruthyunjaya, The Stewart platform manipulator: a review, Mechanism and Machine Theory 35 (2000) 15-40.

[4] S.H. Koekebakker. Model based control of a flight simulator motion system, PhD thesis, Delft University of Technology, 2001.

[5] S.H. Koekebakker. Feedback linearisation of a flight simulator motion system. Journal A, Benelux Quarterly Journal on Automatic Control, 39(2):28–34, 1998.

[6] S.H. Koekebakker, P.C. Teerhuis, and A.J.J. van der Weiden. Multiple level control of a hydraulically driven flight simulator motion system. In Proc. IEEE Systems, Man and Cybernetics IMACS Conf. CESA'98, pages 886–891, 1998.

[7] Davliakos, E. Papadopoulos, Model-based control of a 6-dof electrohydraulic Stewart–Gough platform, Mech. Mach. Theory (2008), doi:10.1016/j.mechmachtheory.2007.12.002.

[8] Li and S.E. Salcudean. Modelling, simulation, and control of a hydraulic Stewart platform. In Proc. IEEE Conf. on Robotics and Automation, pages 3360–3366, 1997.

[9] J.E. McInroy. Dynamic modeling and decoupling force control of a precision hexapod. In Proc. IFAC Workshop on Motion Control, pages 251–256, 1998.

[10] J. E. McInroy and J. C. Hamann, "Design and control of flexure jointed hexapods," IEEE Trans. Robot. Automat., vol. 16, pp. 372–381, Aug. 2000.

[11] Yixin Chen and John E. McInroy, Decoupled Control of Flexure-Jointed Hexapods Using Estimated Joint-Space Mass-Inertia Matrix, IEEE TRANSACTIONS ON CONTROL SYSTEMS TECHNOLOGY, VOL. 12, NO. 3, MAY 2004, pages 413-421.

[12] R. Hoffman. Dynamics and control of a flight simulator motion system. In Proc. Canadian Conference of Automatic Control, 1979.

[13] A.R. Plummer, and P.S. Guinzio, Modal control of an electrohydrostatic flight simulator motion system. In: Proceedings of the ASME Dynamic Systems and Control Conference 2009, DSCC2009. New York: American Society of Mechanical Engineers, pp. 1257-1264.

[14] H.E. Merritt, Hydraulic Control Systems, Wiley, 1967.

[15] H.R. Li, Hydraulic Control Systems, National Defence Industry Press, 1990.

[16] Yang CF, Huang QT, Jiang HZ, Peter OO, Han JW. PD control with gravity compensation for hydraulic 6-DOF parallel manipulator. Mechanism and Machine Theory 2010;45:666–77.

[17] Van Schothorst. Modelling of long-stroke hydraulic servo-systems for flight simulator motion control and system design. PhD thesis, Delft University of Technology, 1997.

[18] Van Schothorst, P.C. Teerhuis, and A.J.J. van der Weiden. Stability analysis of a hydraulic servo-system including transmission line effects. In Proceedings of the Third International conference on Automation, Robotics and Computer Vision, Singapore, pages 1919–1923, 1994.

Hong-zhou JIANG received his B.S. degree from Dalian Jiaotong University, in 1993, and the M.S. and Ph.D degrees in 1996 and 2001, respectively, all from Harbin Institute of Technology.

He is currently a professor of Mechatronics Engineering at Harbin Institute of Technology. His research interests include parallel manipulators, biomimetic robotics, hydraulic control system, system simulation and control system software development.

Jing-feng HE received his B.S. degree in 1997, the M.S. and Ph.D degrees in 2001 and 2007, respectively, all from Harbin Institute of Technology.

He is currently an associate professor of Mechatronics Engineering at Harbin Institute of Technology. He researches on parallel manipulators with redundant actuation, optimal design and fault-tolerant parallel manipulators.

Zhi-zhong TONG received his B.S. degree in 2001, the M.S. and Ph.D degrees in 2003 and 2007, respectively, all from Harbin Institute of Technology.

He is currently a lecturer of Mechatronics Engineering at Harbin Institute of Technology. His research interests are in the areas of parallel manipulators, robotic dynamics and biomimetic robotics.